J Appl Electrochem (2011) 41:939–949
DOI 10.1007/s10800-011-0319-7

ORIGINAL PAPER

High throughput systems for screening biomembrane interactions on fabricated mercury film electrodes

Zachary Coldrick · Abra Penezić · Blaženka Gašparović · Paul Steenson · Jon Merrifield · Andrew Nelson

Received: 4 January 2011 / Accepted: 18 April 2011 / Published online: 13 May 2011

Abstract A sensing system for the rapid *on-line* screening of lipids and biomembrane active compounds in water samples has been successfully developed. The sensor consists of a flow cell and incorporated wafer-based device with *on-chip* mercury on platinum (Pt/Hg) working electrode and platinum (Pt) auxiliary and pseudo-reference electrodes. To optimise system performance, the following experiments were carried out: (i) Deposition and removal of phospholipid layers on and from Pt/Hg electrodes respectively, (ii) Effect of electrode size on signal, (iii) Monitoring of different phospholipids deposited in flow cell and, (iv) Detection of phospholipid monolayer interaction with representative compounds. The results showed that: (i) Miniaturisation and ruggedisation of the mercury (Hg)/phospholipid system has been successfully achieved, (ii) Rapid cyclic voltammetry facilitates repetitive dioleoyl phosphatidylcholine (DOPC) monolayer formation on Hg from aqueous DOPC dispersion and, (iii) The device responds selectively to organic compounds injected into electrolyte flow.

Z. Coldrick · A. Nelson (✉)
Centre for Molecular Nanoscience (CMNS), School of Chemistry, University of Leeds, Leeds LS2 9JT, UK
e-mail: a.l.nelson@leeds.ac.uk

A. Penezić · B. Gašparović
Rudjer Boskovic Institute, Centre for Marine and Environmental Research, POB 180, 10002 Zagreb, Croatia

P. Steenson
School of Electronic Engineering, University of Leeds, Leeds LS2 9JT, UK

J. Merrifield
Organisense Ltd, Leeds Innovation Centre, Leeds LS2 9DF, UK

Keywords Flow cell · Mercury film electrode · Wafer based sensing device · Phospholipid monolayer · Adsorption/desorption

1 Introduction

The phospholipid coated mercury (Hg) electrode has had considerable application in studying the fundamental properties of phospholipid layers in an electric field [1–4]. In addition to this, the system has been used as a biological membrane model for analysing ion channel function and co-enzyme electron transfer [5, 6]. However, its main strategic application is its use as a sensor for biological membrane active compounds [7–9]. The reason for this is that the fluidity of the phospholipid layers is entirely complimentary with the smooth Hg surface. This fluidity is registered in the capacitance-potential trace as very sharp discontinuities in the capacitance as the applied potential is ramped to more negative values [3, 9, 10]. It has been shown that compounds (such as cholesterol) which interact with the phospholipid layer affect its structure and fluidity [2] and accordingly change the nature of the capacitance discontinuities which represent electrically-induced phase transitions. Although such changes are highly reproducible and quantitative, their application in sensor development has been severely restricted by the fragility and inaccessibility of the hanging Hg drop electrode (HMDE) [11] which has traditionally been used as a support for the phospholipid layers [1–8].

Attempts to transfer the Hg-phospholipid system to a more robust platform have necessitated the replacement of the HMDE with microfabricated Hg film electrodes as a support for the phospholipid layer. A previous paper has shown that wafer-based Hg film electrodes were successful

at supporting phospholipid layers in a stable and reproducible configuration [9]. In addition, the renewability of the HMDE was maintained by the ability to electrochemically clean and regenerate the Hg film surface. This advance represented a major innovation, namely the improved manipulability and accessibility of the Hg electrode for adsorbed organic layer studies. The Hg film electrodes described previously [9] were however not ideally suited to high throughput analysis of samples and required a relatively large electrochemical cell containing a macroscopic reference electrode and a platinum (Pt) bar auxiliary electrode to operate. Preliminary work [9] had shown that Pt based Hg film (Pt/Hg) electrodes could be used in a flow cell enabling experiments to be carried out more rapidly and electrode regeneration to be accomplished more effectively. The original silicon (Si) wafer-based electrode's design was such that it was difficult to seal within a flow cell and render the assembly water tight. Other problems associated with the micro silver/silver chloride (Ag/AgCl) reference electrode employed namely a blocked frit resulted in an unacceptable drift in reference potential and in extreme cases loss of reference potential resulting in damage to the Pt/Hg electrode. These effects necessitated a redesign of the device for its use as an *on-line* high throughput sensing system.

Sensors based on the transduction of phospholipid bilayer and monolayer responses to analytes in solution have been anticipated for some time [12–14]. However, the problems associated with the use of free standing bilayers in sensors have always been associated with their mechanical and electrical fragility [15, 16]. This has been solved to some extent by the deployment of supported [17] and suspended [18] bilayer and monolayer/bilayer [19] devices as putative sensor systems. Nonetheless, these developments have become unnecessarily complicated to use as simple detection systems in spite of their biological relevance [20, 21]. In fact their complexity is related to their configuration and the mechanisms involved in the sensing which involve some kind of binding system [20, 21]. The phospholipid on Hg system occupies a unique niche among membrane-based sensors and has received considerable scientific interest [22]. The reason for this is that the detection of biomembrane active compounds by the Hg/phospholipid device through the effect of the compounds on the phospholipid phase transitions [9] is inherently simple, elegant and biologically relevant [23, 24]. Indeed the properties of the phospholipid coated Pt/Hg film electrode together with its proposed transfer from a macroscopic electrochemical cell to a high-throughput *on-line* sampling system makes it one of the first field-compatible membrane-based sensors available for the rapid and reproducible detection of biomembrane type interactions on electrode surfaces. The miniaturisation and ruggedisation of the detection system to this end is detailed in the following steps in this paper:

(i) The design of microfabricated Pt/Hg film electrodes with *on-chip* auxiliary and pseudo-reference electrodes.
(ii) The design of a flow cell incorporating the microfabricated Pt/Hg film electrode.
(iii) The use of flow injection systems for phospholipid deposition and sampling.
(iv) The optimisation of potential controlled deposition and removal of phospholipids on and from respectively Pt/Hg film electrodes.

2 Experimental

2.1 Rapid cyclic voltammetry (rcv), *on-chip* electrodes and flow cells

Microfabricated wafer-based devices (WBD) shown in Fig. 1a were of four designs including eight Pt disc working electrodes of identical radii (500, 250, 100, or 50 μm) and two rectangular Pt electrodes: a pseudo-reference and auxiliary electrode. The design incorporated ten Pt contact pads interfaced with an Autolab PGSTAT12 potentiostat (Ecochemie, Utrecht, The Netherlands). The metal traces connecting the pads to the electrodes were insulated by $\sim$0.5 μm thick Si_3N_4. The electrodeposition of Hg on to the eight Pt disc electrodes on the installed WBD was performed in an open cell (Fig. 1b) [9]. The amount of Hg electrodeposited on to each electrode together with the charge passed is displayed in Table 1. Following electrodeposition, the capacitance of the Pt/Hg electrodes was measured using rcv [9] at ramp rates >10 V s^{-1}. The potentiostat was interfaced to a Powerlab 4/25 signal generator (AD Instruments Ltd). The rcv current is linearly related to the capacitance of the electrode/electrolyte interface in the absence of a faradaic reaction. In the presence of traces of oxygen from air in the flow cell, oxygen reduction appeared as a small broad faradaic current in addition to the capacitance current. rcv was used [9] to determine the surface area of the uncoated Hg/electrolyte interface and to characterise phospholipid interactions on the electrode surface.

The significant potential drift of the Ag/AgCl:3.5 mol dm^{-3} KCl micro-reference electrode in the preliminary flow cell [9] prompted the use of Pt as a pseudo-reference electrode which is enabled by the patterning of the Pt reference on to the Si wafer. This *on-chip* reference has none of the disadvantages associated with a blocked frit or secondary internal reference solution and is close to the working electrodes. The disadvantage of using a Pt pseudo-reference electrode is that its reference potential

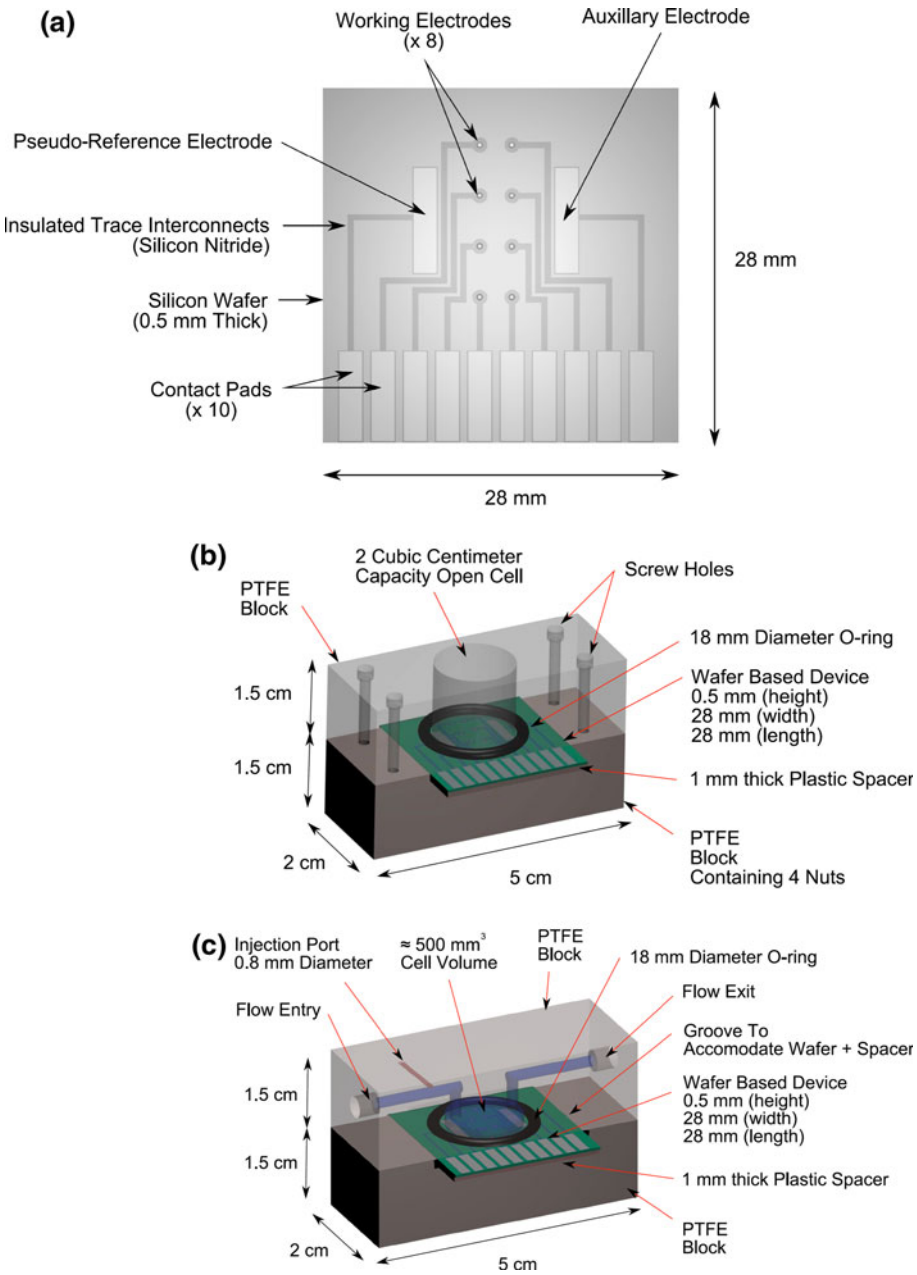

Fig. 1 3D schematic diagrams of: **a** The wafer-based device (WBD) design incorporating eight Pt disc electrodes and two rectangular Pt electrodes each individually addressed via Si_3N_4-insulated interconnects to 2.54 mm pitch Pt contact pads. **b** A static electrochemical cell. **c** A flow cell with screw holes omitted for clarity designed to accommodate the 28 mm^2 WBD

Table 1 Electrode areas of Pt/Hg discs calculated from their capacitance in 0.1 mol dm^{-3} PBS, pH 7.4 measured at 40 V s^{-1} on the "water hump" local current maximum

Electrode radius (μm)	Pt disc area (mm^2)	Charge passed to electroplate Hg (C)	Deposited Hg mass (mg)	Mean "water hump" capacitance current (μA) SD for $n = 3$	Estimated area (mm^2)
500	0.786	1	1	13.6	0.851
				SD 0.123	SD 0.0086
250	0.196	0.125	0.13	3.68	0.23
				SD 0.0135	SD 0.0090
100	0.0314	0.008	0.008	0.814	0.051
				SD 0.00578	SD 0.00036
50	0.00786	0.001	0.001		

Charge in coulombs (C) required to deposit given mass of Hg on Pt shown

varies with the electrolyte composition and concentration and when the electrode becomes contaminated. This can be alleviated by calibrating the reference potential versus the potential value of the voltammetric peaks of dioleoyl phosphatidylcholine (DOPC) on Hg [9]. The pseudo-reference electrode contamination can be minimised by maintaining a continuous flow of electrolyte over the electrode. The potential of the *on-chip* evaporated Pt pseudo-reference electrode was measured relative to a standard Ag/AgCl:3.5 mol dm^{-3} KCl reference electrode using a static cell similar to the one in Fig. 1b with a Ag/AgCl electrode above the WBD in contact with the electrolyte. A 500 μm Pt/Hg working electrode uncoated and coated with DOPC was used and the rcv scan was recorded against the Ag/AgCl reference electrode and the Pt pseudo-reference electrode respectively.

Pt electrodes have been proposed previously as reference electrodes in situations where conventional reference electrodes cannot be used [25]. These electrodes were found to exhibit a constant potential about 300 mV more positive than that of the Ag/AgCl:sat'd KCl electrode. Other studies showing a similar potential of the Pt reference electrode have attributed its potential to a rather complicated Nernstian reaction involving the oxidation of Pt [26]. The use of Pt wire as reference electrode is often referred to as a pseudo-reference electrode which has a constant potential with unknown origin where the potential varies according to the solution composition and concentration [27]. Accordingly, the Pt reference in this study is referred to as a pseudo-reference electrode. Unless stated otherwise, all electrochemical measurements reported in this paper were carried out using the Pt pseudo-reference electrode and all quoted potentials are related to its potential.

To characterise phospholipid interactions, the WBD was installed inside the flow cell (see Fig. 1c). A constant stream of pH 7.4 phosphate buffered saline (PBS) of composition; 0.1 mol dm^{-3} KCl (calcined at 600 °C) and 0.01 mol dm^{-3} phosphate [9], sourced from a 5 dm^{-3} capacity reservoir, was passed over the electrode surface. A flow rate of 5 cm^3 min^{-1} pumped by a peristaltic pump with pumpsil 913 A016.016 peristaltic tubing (Watson Marlow, UK) was used. The flow cell contained a sampling port upstream of the WBD (Fig. 1c) for the injection of phospholipid dispersions/samples. The PBS electrolyte in the reservoir was de-aerated by sparging with argon. 2 mg cm^{-3} dispersions of DOPC, dioleoyl phosphatidylglycerol (DOPG), dioleoyl phosphatidylserine (DOPS) and dioleoyl phosphatidylethanolamine (DOPE) (Avanti-lipids, USA) in PBS were prepared by adding the phospholipid directly to PBS electrolyte with agitation. In the bulk of such dispersions, the phospholipid exists as vesicles or micelles [28] but without a defined liposome size and/or lamella thickness. Coatings of each phospholipid were deposited successively on the Pt/Hg electrode in the flow cell (Fig. 1c) by injecting 50 μdm^3 of each phospholipid dispersion therein. Phospholipid deposition was monitored while applying rcv from −0.4 to −3 V at 100 V s^{-1} [9]. The preferred level of coverage was selected by opening the circuit when the voltammetric peak corresponding to the first reorientation phase transition reached a maximum current value which is characteristic of monolayer coverage for each specific phospholipid [9]. Coatings of DOPC, DOPE, DOPG, and DOPS were deposited as described above and monitored by rcv at 40 V s^{-1} from −0.4 V to potentials equal to and more negative than −1.6 V (DOPC, DOPE) and from potentials −0.4 to −1.4 V (DOPG, DOPS) [9]. The Pt/Hg electrode was electrochemically cleaned as reported earlier [9].

2.2 Different sized electrodes and spreading and removal of phospholipids

The surface area of three of the electrode sizes with electrodeposited Hg were obtained from the "water hump" current at approximately −0.5 V on uncoated electrodes [9] and are displayed in Table 1. These area values were used for all calculations of flux (J) and capacitance (C) of the coated electrodes. The small faradaic current from the trace oxygen reduction did not interfere with the surface area measurements since it occurred at potentials more negative than the "water hump" capacitance current. rcv scans were recorded over a potential range of −0.4 to −1.8 V at 200 V s^{-1} for DOPC coated devices of radii 500, 250, 100 and 50 μm. The system's parasitic capacitance current was measured while not addressing any working electrodes over the interrogation potential ranges and this current was subtracted from the current data.

Experiments were carried out in the static cell open to the air (see Fig. 1b) with the 500 μm radius Pt/Hg electrode to look at the concentration of DOPC in dispersion necessary for successful coating of the Pt/Hg electrode. Solutions of DOPC in PBS were prepared in the following concentrations; 4, 2, 1, 0.2, 0.02, 0.01, 0.008, 0.004, 0.002 and 0.0002 mg cm^{-3}. Each dispersion was independently added to the cell. The single 500 μm Pt/Hg electrode was addressed as working electrode using the separate *on-chip* Pt auxiliary and pseudo-reference electrodes. 100 consecutive rcv scans over the potential range of −0.4 to −3 V at 130 V s^{-1} for one minute were recorded. To investigate the influence of applied potential on phospholipid deposition, a 500 μm radius Pt/Hg electrode plus Ag/AgCl: 3.5 mol dm^{-3} KCl reference centred above the WBD in contact with the PBS electrolyte and Pt auxiliary *on-chip* electrodes in the flow cell shown in Fig. 1c were used. 150 μdm^3 of a DOPC dispersion was injected into the flow

cell. The electrode potential was held at a single potential in the range of −0.4 to −2.5 V (in 0.1 V steps) for 2.5 min while the DOPC dispersion passed over the electrode surface. The surface was monitored for phospholipid adsorption after the time period by applying rcv. Finally, the effect of applied potential on the desorption process was measured using a 500 μm radius Pt/Hg mercury film electrode coated with a DOPC layer in the flow cell (Fig. 1c). Potentials were measured using the *on-chip* Pt pseudo-reference electrode. The reproducibility and integrity of the deposited layer was checked using rcv. Subsequently, the electrode potential was stepped from −0.4 V where the DOPC layer has maximum stability [29] to potentials in the range of −1.8 to −3 V in steps of 0.1 V and held for 100 ms to 20 s. After each pulse the electrode surface was checked for DOPC desorption using rcv.

2.3 Sensor exemplification

Figure 2 displays the sensing device set-up (Fig. 2a) and operation (Fig. 2b). The effect of 3-(2-chloro-10*H*-phenothiazin-10-yl)-*N*,*N*-dimethyl-propan-1-amine (chlorpromazine) in a natural water matrix was tested for interaction with the 500 μm diameter DOPC coated Pt/Hg electrode in the flow cell. 1 cm^3 of a water sample sourced from a local stream (Wells Walk, Ilkley, North Yorkshire), unspiked and spiked with 1 μmol dm^{-3} chlorpromazine (SigmaAldrich)) was injected into the flow cell. The rcv of the layer was recorded both before and 20 s after chlorpromazine injection. A series of apolar compounds were also investigated in respect of their monolayer activity. These compounds were: pyrene, 1,1,1-trichloro-2,2-bis-(*p*-chlorophenyl) ethane (DDT), 2,4,5-trichlorophenoxyacetic acid (TCA), and 2,4-dinitrophenol (DNP) (SigmaAldrich). Samples were prepared in serial tenfold dilutions from 10 mmol dm^{-3} to 1 nmol dm^{-3} in methanol except for dinitrophenol which was prepared in water. 100 μdm^3 of sample solution was slowly injected into the flow cell, and a rcv was recorded 20 s after injection. Experiments for each concentration were performed three times to allow for any error. Control experiments were performed, where methanol was added to the flow system, in the same quantities, as the solutions containing the compounds. In spite of the electrolyte de-aeration, some air was adventitiously introduced into the system through tubing/connectors and with the injection of solution into the flow cell.

3 Results and discussion

Figure 3a and b shows the rcv scans of a single uncoated and DOPC coated 500 μm radius Pt/Hg electrode measured against the Ag/AgCl: 3.5 mol dm^{-3} KCl reference

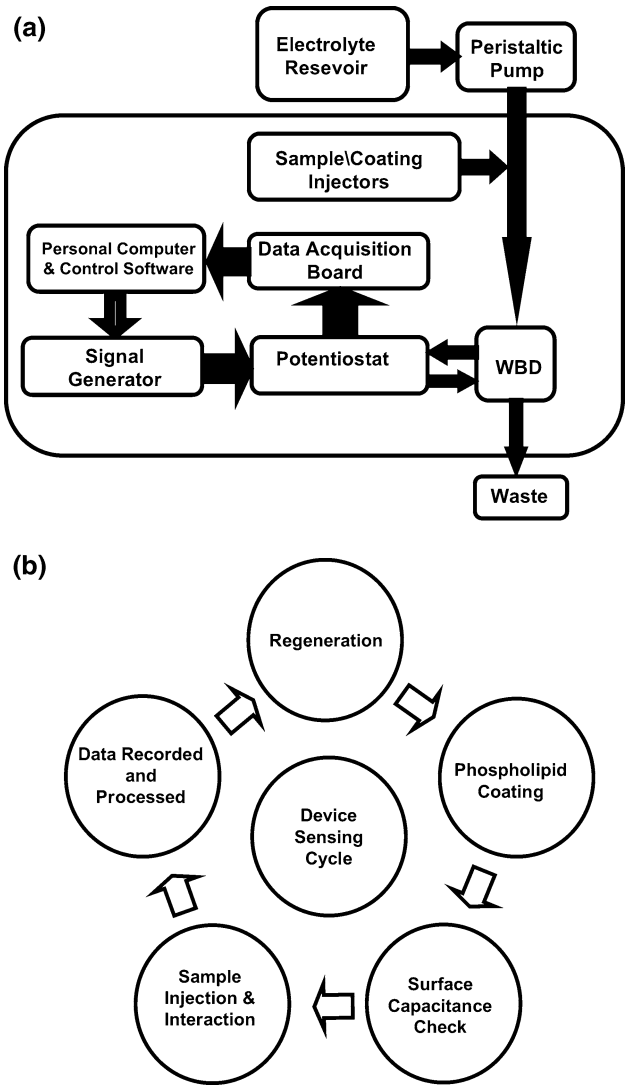

Fig. 2 **a** The control system of the flow cell based sensing device with computer controlled pathways, current data acquisition pathways, and electrolyte flow represented by arrows respectively. **b** A flow cycle of the sensing process

electrode and, separately the *on-chip* evaporated Pt pseudo-reference electrode. Of particular significance is the negative potential shift of the "water hump" (Fig. 3a) and the voltammetric peaks (Fig. 3b) recorded versus the Pt reference electrode by ∼200 mV compared to the same scans recorded versus the Ag/AgCl reference electrode. These results show that the potential of the fabricated Pt pseudo-reference electrode is ∼200 mV positive from that of the Ag/AgCl electrode. This potential shift is of a similar magnitude to that (∼300 mV) recorded in the literature for a Pt reference electrode [25]. The first and second voltammetric peaks in the rcv scan on the DOPC coated electrode (Fig. 3b) are separated by 100 mV on both of the traces recorded with each reference electrode. This indicates that both traces are equivalent and there is no

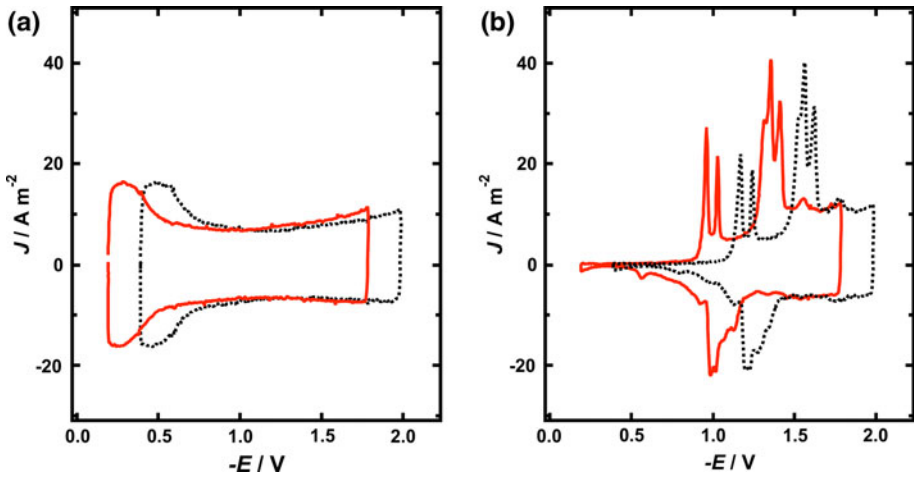

Fig. 3 rcv scans with current normalised as flux (J) by the electrode surface area, of a 500 μm radius Pt/Hg electrode recorded at 40 V s^{-1} in a flow cell (PBS flow of 5 cm^3 min^{-1}) with a central Ag/AgCl:3.5 mol dm^{-3} KCl reference electrode in addition to the *on-chip* Pt reference electrode. rcv scans were recorded for: **a** the clean Hg surface and, **b** the DOPC coated Pt/Hg electrode versus the Ag/AgCl reference (*solid line*) and versus the *on-chip* Pt pseudo-reference (*dotted line*)

potential distortion observed carrying out the measurements versus the Pt pseudo-reference electrode. The results validate the use of a fabricated Pt film as a reference electrode which offers many advantages over the Ag/AgCl system. The findings are consistent with previous recommendations concerning its use [25–27]. A factor which contributes to its stability as a reference electrode in this study is its large surface area (see Fig. 1a) exploited also in the nanoporous reference electrode of Han et al. [26]. Results have also shown however that the potential of the pseudo-reference electrode can drift when it becomes contaminated with organic material during use. This is solved by the in situ washing of the electrode in the flow cell with a small quantity of acetone.

Figure 4 displays the real time scans of phospholipid adsorption as a function of phospholipid dispersion concentration in contact with the electrode with applied potential cycling (−0.4 to −3 V) in a static cell open to the air. At the low concentration of 0.0002 mg cm^{-3} DOPC in PBS, the electrode remains uncoated as exemplified by the rcv scan profile typical of a clean Hg surface in the presence of oxygen (Fig. 4d). If the DOPC concentration is increased to 0.010 mg cm^{-3}, then the current peaks characteristic of the DOPC layer appear. These peaks exist for a number of successive scans before collapsing due to the layer desorbing. The layer periodically re-spreads during the 100 scans (Fig. 4c). The re-spreading occurs with periodicity and at the DOPC concentration of 0.010 mg cm^{-3} the re-spreading period is approximately every 10 s. Increasing the DOPC dispersion concentration to 0.2 mg cm^{-3} pushes the equilibrium between the adsorbed phospholipid layer and phospholipid dispersion in the direction of the adsorbed layer (see Fig. 4b). Figure 4a shows that in the presence of 4 mg cm^{-3} DOPC, the rcv scan of the Pt/Hg electrode is characteristic of the over-coated layer state with a depression of the voltammetric peaks. Figures 4a and b show that despite the 100 scans to −3 V, the layer appears not to be desorbed. As a result the

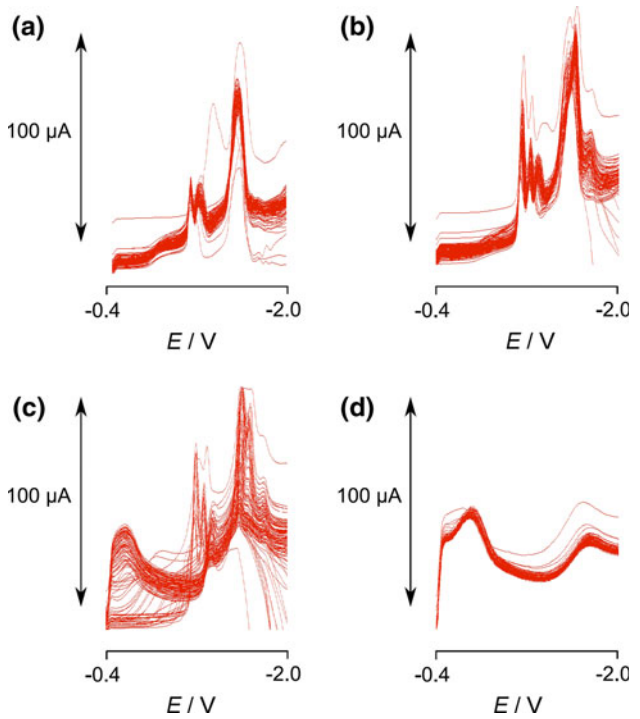

Fig. 4 rcv scans recorded at 130 V s^{-1} over the range −0.4 to −3 V, 100 consecutive scans overlaid (~4.5 scans per second), of a 500 μm radius Pt/Hg electrode in DOPC dispersions of: **a** 4, **b** 0.2, **c** 0.01, and **d** 0.0002 mg cm^{-3} in PBS in a static electrochemical cell. Potentials (E) quoted versus Pt pseudo-reference electrode

concentration of DOPC in the dispersion of 2 mg cm^{-3} routinely injected into the flow cell is ten times that necessary (0.2 mg cm^{-3}) to ensure full coverage of the electrode in the absence of flow. Under routine analytical conditions, the presence of flow and the limited time contact of the electrode with the dispersion prevents the formation of an over-coated layer on the Pt/Hg.

It has been shown that the adsorption/spreading process of phospholipids on Hg is due to the negative polarisation of the electrode surface aiding the disruption of micelles/vesicles lowering the energy required to do this [30, 31]. Figure 5a shows that when the electrode is held at −0.4, −0.9 and −1.8 V versus the Ag/AgCl:3.5 mol dm^{-3} KCl reference electrode for 2.5 min in the presence of a DOPC

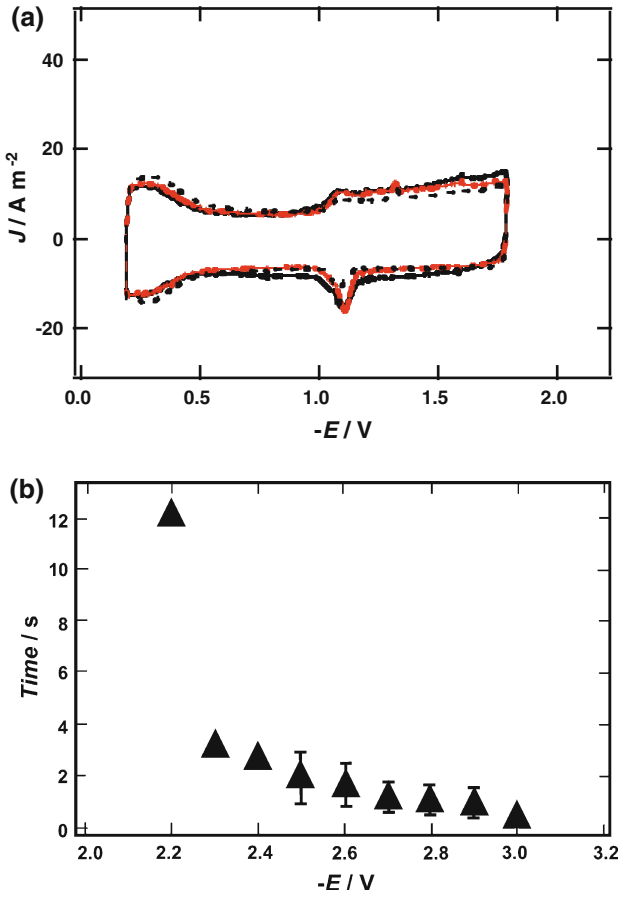

Fig. 5 **a** rcv scans with current normalised as flux (*J*) by the electrode surface area, of a 500 μm radius Pt/Hg electrode recorded at 40 V s^{-1} in a flow cell (PBS flow of 5 cm^3 min^{-1}). rcv scans recorded following 2.5 min exposure to injection of 150 μdm^3 of a DOPC dispersion of 2 mg cm^{-3} into the flow cell at applied potentials of: (*solid line*) −0.4 V, (*red/greyscale line*) −0.9 V and (*dashed line*) −1.8 V. All quoted potentials (*E*) were measured versus the Ag/AgCl:3.5 mol dm^{-3} KCl reference electrode. **b** Time (s) required to remove DOPC from 500 μm radius Pt/Hg electrode in 0.1 mol dm^{-3} PBS electrolyte at flow 5 cm^3 min^{-1} plotted against the applied potential (*E*) on the electrode measured versus Pt pseudo-reference electrode

dispersion vesicle flow, a subsequent rcv scan (−0.2 to −1.8 V versus the Ag/AgCl:3.5 mol dm^{-3} KCl reference electrode at 40 V s^{-1}) of the electrode shows no significant adsorption of phospholipids, and a depressed capacitance "water hump" prevails. On the other hand, it has been observed in Figs. 3b and 4 that phospholipids adsorb and spread on to the Pt/Hg electrode while the potential is being cycled between −0.4 and −3 V at 100 V s^{-1}. Accordingly the rapid potential scanning facilitates the formation of DOPC layers on the Pt/Hg electrode in electrolyte flow.

Figure 5b is a plot of the time required for DOPC removal to occur plotted against the potential of the step using the procedure described in Sect. 2.2. Potentials more positive than −2.2 V required longer than 200 s to remove the DOPC from the electrode surface. It can be seen that the time of desorption is influenced by the extremity of the negative potential applied. It is concluded therefore that the DOPC removal process is not limited solely by the diffusion of DOPC from the surface at potentials more negative than those characterising the desorption peaks. The short desorption time of less than 0.1 s at −3 V observed in Fig. 5b is concurrent with the necessary use of the rcv excursion to this potential in removing the DOPC layer from the electrode surface. This phospholipid removal from the electrode surface can be facilitated by polarisation, potassium ion reduction/amalgamation and hydrogen evolution or a combination of each process, and the mechanism thereof is currently being investigated.

It can be construed from previous findings [10, 29, 32, 33] that DOPC assemblies in dispersion can adsorb on the Hg surface at potentials between −1.4 and −0.9 V during a positive going potential ramp. This is because in the potential window of −1.4 to −0.9 V, DOPC vesicles and/or bilayer patches and/or DOPC emulsions depending on the potential are energetically stable on the Hg surface [10, 29, 32, 33]. The DOPC assembly adsorption will not involve spreading of the DOPC monolayer on the electrode surface. However, a continuation of an applied voltage ramp to −0.4 V will allow the adsorbed DOPC assemblies to convert to a monolayer [10, 29, 32, 33]. Such a mechanism is depicted for dimyristoyl phosphatidylcholine (DMPC) adsorption in Fig. 4 of ref [30]. A repetition of this process during rcv, where the concentration of DOPC in the dispersion (0.2 mg cm^{-3}) inhibits a net DOPC desorption, leads to the repetitive formation and build up of a stable fully covered monolayer.

Figure 6 displays the rcv scans obtained from the DOPC coated Pt/Hg electrodes of different dimensions. A higher scan rate of 200 V s^{-1} was used to enhance the capacitance current which caused the capacitance peaks to broaden somewhat. A sharp voltammetric peak profile can be observed on 100 μm radius electrodes although on smaller 50 μm radius electrodes a considerable background current

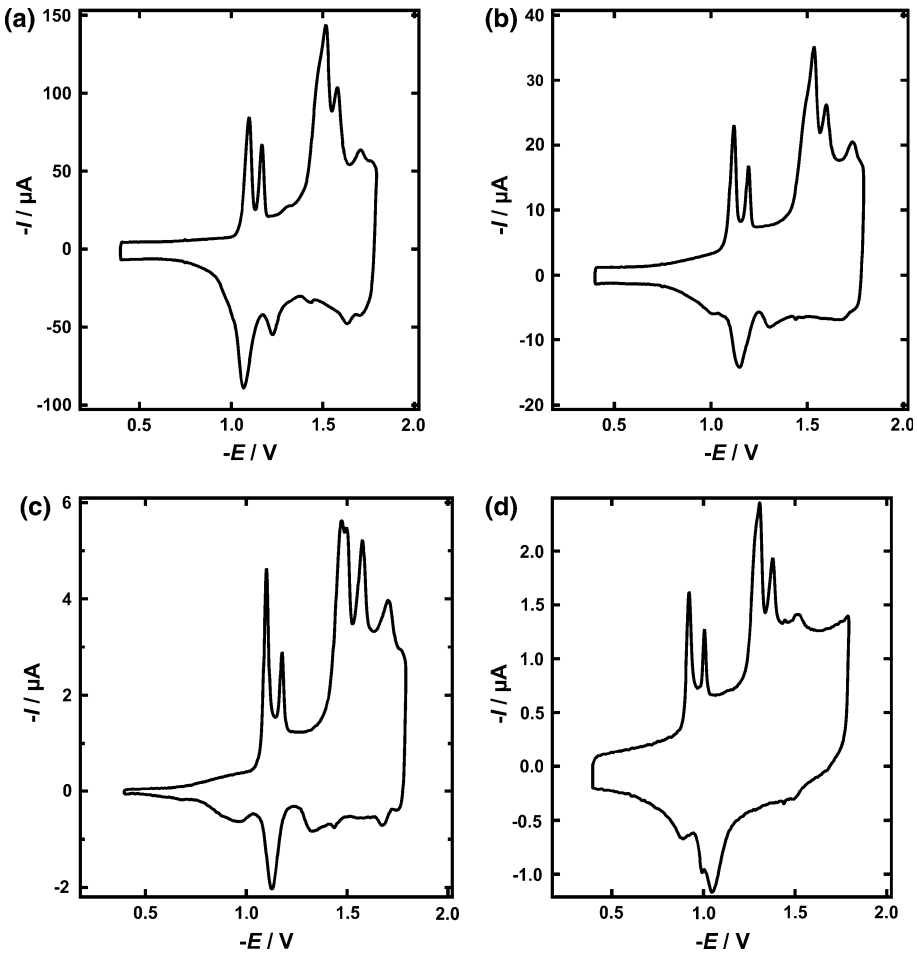

Fig. 6 rcv scans recorded at 200 V s^{-1}, with system internal parasitic capacitance current subtracted, at single DOPC coated Pt/Hg electrodes of radii, **a** 500 μm, **b** 250 μm, **c** 100 μm and **d** 50 μm. All plots recorded in 5 cm^3 min^{-1} PBS electrolyte flow versus Pt pseudo-reference electrode

begins to interfere with the signal even after baseline correction. The slope apparent on the rcv scans of the DOPC coated smaller dimension electrodes indicates that faradaic reduction processes of trace oxygen reduction and at more negative potentials peroxide reduction contribute to a greater proportion of the total current signal for these electrodes. This is a result of radial diffusion of oxygen to these microelectrodes which will contribute proportionately more current than linear diffusion to the same area electrode. In the case of radial diffusion to microelectrodes [34], the flux to the microelectrode is greater than the flux to larger area electrodes because the region from which electroactive species diffuse to the surface is in essence hemispherical in shape. The interference of faradaic processes on the rcv scan of the uncoated 50 μm Pt/Hg electrodes prevented the surface area of these electrodes being determined (Table 1).

Figure 7 shows the rcv scans of four respective phospholipids each deposited on the microfabricated Pt/Hg electrodes. The cathodic arms of the plots are very similar to those observed in Fig. 6 of the previous study [9] which was carried out in a static glass cell containing 75 cm^3 electrolyte and using a standard Ag/AgCl reference electrode. The cathodic arms of the rcv scans of the phospholipid: DOPC, DOPE, DOPG and DOPS coated Pt/Hg electrode show the characteristic finger-print voltammetric profiles specific to these phospholipids. In addition to the desorption peak(s) at the most negative potentials, these profiles consist of the characteristic twin voltammetric peaks of DOPC, the single voltammetric peak of DOPE, the closely spaced voltammetric peaks of DOPG and the single voltammetric peak at more negative potentials of DOPS. The results in Fig. 7 represent an advance since in the flow cell only small volumes (0.5 cm^3) of electrolyte are used and deposition is by adsorption from phospholipid dispersion under potential cycling control unlike adsorption at the gas/electrolyte interface in the static cell. The results in Fig. 7 establish the flow cell as an alternative and valid technique for depositing and screening phospholipid layers on Pt/Hg electrodes.

Figures 8a and b display the results of interaction of the biomembrane active pharmaceutical [9] chlorpromazine with the DOPC layer added to a natural water matrix. It is seen that the natural water matrix itself has no effect on the voltammetric profile of the phospholipid layer. On the other hand, when the natural water is spiked with the

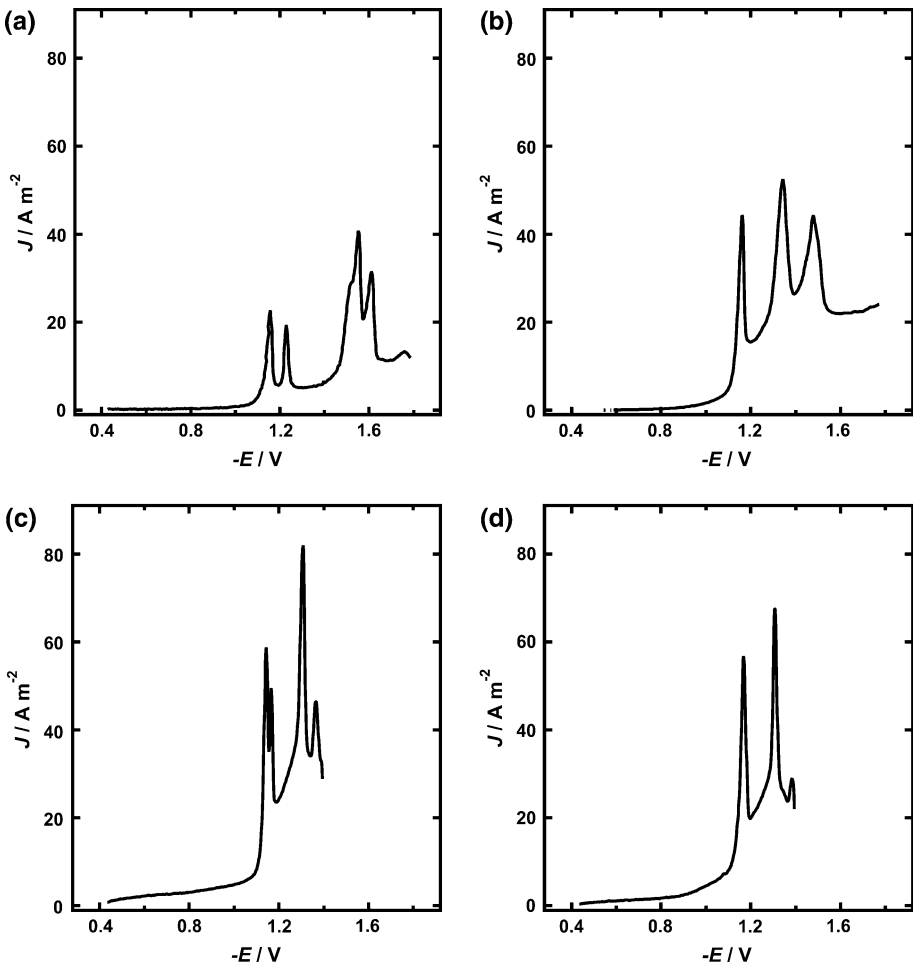

Fig. 7 Cathodic arms of rcv scans recorded at 40 V s^{-1} from 500 μm radius Pt/Hg electrodes versus Pt pseudo-reference electrode on a WBD in PBS (flow rate: 5 cm^3 min^{-1}) in the flow cell with current normalised as flux (*J*) by electrode surface area with phospholipid layers formed from dispersions of, **a** DOPC, **b** DOPE, **c** DOPG and, **d** DOPS

chlorpromazine and injected into the flow system, a clear interaction is observed. The most significant feature of these results is that they show that the flow cell and incorporated WBD can be used to routinely assay the biomembrane activity of a flow injected compound in a natural water sample. The broad oxygen reduction wave arising from traces of air introduced with the sample injection does not interfere with the capacitance current peaks or their suppression.

Figures 8c, d, e and f show the effects of representative apolar compounds on the device response. The cathodic arm of the rcv is only displayed within potentials bounding the two voltammetric peaks used as an indicator of interaction for clarity. It is significant to note that each compound following interaction with the sensing DOPC monolayer shows a different and characteristic response. The response increases with increase in concentration of compound in the working solution which is injected into the flow. The response to pyrene and DDT is identical to the effect of pyrene [7, 35] and DDT [7, 35, 36] interaction respectively on the voltammetric curve of a DOPC coated HMDE in a 75 cm^3 electrochemical cell. The effect of pyrene interaction induces the negative potential shift, potential separation and suppression of two voltammetric peaks whereas the effect of DDT interaction is to elicit a suppression of the voltammetric peaks. The individual sensitivities are also significant and are clearly related to the hydrophobicity and aromaticity of the tested compound [36]. The sensor's responses to pyrene and DDT are commensurate with these compounds having the highest log octanol/water ($logP_{OW}$) partition coefficients of 5.22 for pyrene [37] and 6.2 for DDT [38] The decreased sensor's responses to TCA and DNP are also in accord with these compounds' $logP_{OW}$ values which are 0.31 for TCA [39] and 1.67 for DNP [40]. The determination of an absolute detection limit is not possible with the present design of the system which requires an additional circulation loop to allow the passing of a defined electrolyte concentration of compound over the device. Such an improvement in design of the sensing system is currently being implemented.

4 Conclusions

The present study has achieved (a) the successful miniaturisation of the phospholipid on Pt/Hg system, (b) the

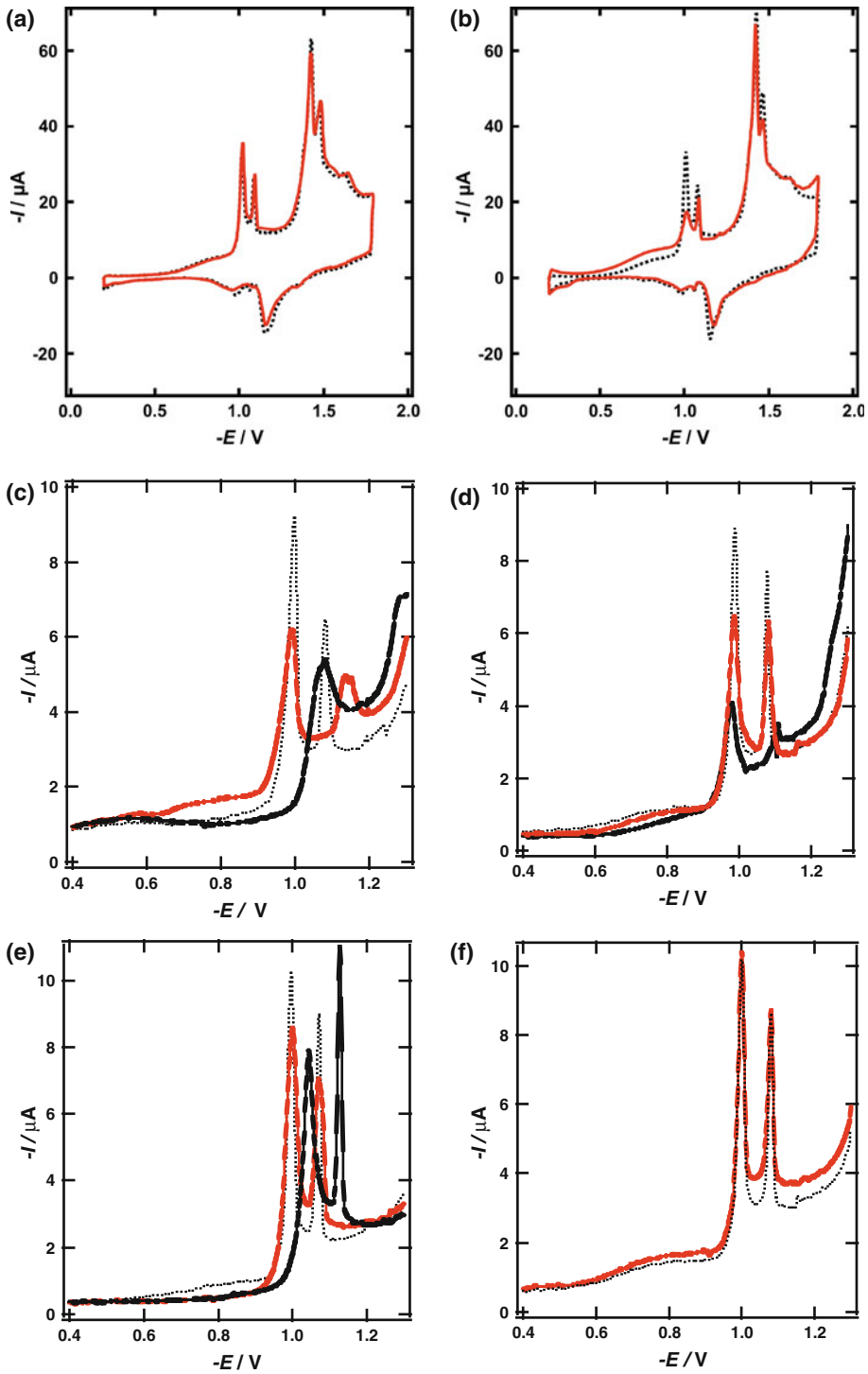

Fig. 8 rcv scans recorded at 40 V s^{-1} from a 500 µm radius DOPC coated Pt/Hg electrode in 5 cm^3 min^{-1} PBS electrolyte flow immediately following injection of 1 cm^3 of MilliQ water (*broken line*) in **a** and **b** and a water sample sourced from a local stream (*solid line*) which was **a** unspiked and, **b** spiked with 1 µmol dm^{-3} chlorpromazine. Cathodic arms of rcv scans recorded at 40 V s^{-1} from a 250 µm radius DOPC coated Pt/Hg electrode in 5 cm^3 min^{-1} PBS electrolyte flow, 20 s following injection of 100 µdm^{-3} methanol (*stippled line*) and 100 µdm^{-3} methanol, **c** 10 µmol dm^{-3} (*red/greyscale line*) and 1 mmol dm^{-3} (*black line*) pyrene, **d** 10 µmol dm^{-3} (*red/greyscale line*) and 10 mmol dm^{-3} (*black line*) DDT, **e** 1 (*red/greyscale line*) and 10 (*black line*) mmol dm^{-3} TCA and, **f** (*red/greyscale line*) 1 mmol dm^{-3} DNP. All potentials (*E*) measured versus Pt pseudo-reference electrode

optimisation of phospholipid deposition on Pt/Hg and, (c) the application of the device to measure selectively the interaction of surfactant and apolar compounds with the phospholipid. These conclusions are described in more detail in the following.

The phospholipid on Pt/Hg system has been successfully transferred to a small volume flow cell where the phospholipid monolayers are deposited under potential control from a dispersion. The use of *on-line* flow injection techniques for phospholipid dispersions and samples and the use of *on-chip* Pt auxiliary and pseudo-reference electrodes greatly speeds up the assay to not more than 10 minutes per sample.

DOPC can only be successfully deposited on to a Pt/Hg electrode from a dispersion concentration equal to and >0.2 mg cm^{-3} when a potential cycling program of

$\sim$100 V s^{-1} is applied with excursion −0.4 to −3 V. It can be interpreted from this that during rcv, the positive going potential scan applied to the Hg/electrolyte interface facilitates repetitive DOPC monolayer formation on Hg from aqueous dispersion. In addition, the most rapid removal of DOPC is obtained when extreme potentials of −3 V are applied to the electrode in electrolyte flow, which is implemented during rcv excursion to this potential.

rcv plots of DOPC, DOPE, DOPG and DOPS coated Pt/Hg electrodes in the flow cell following deposition from dispersion are very similar to those obtained on the coated Pt/Hg electrode in a large volume static cell following deposition from phospholipid layers at the gas/electrolyte interface. The system has been shown to effectively detect the phospholipid monolayer modifying ability of a biomembrane active compound, chlorpromazine, in a natural stream water sample. The effect of a series of apolar aromatically based compounds on the device response is identical to that seen on a DOPC coated HMDE in a macroscopic electrochemical cell and is specific to each compound.

Acknowledgments Funding for this work was provided by the Engineering, Physical and Science Research Council (EPSRC) Grant Reference EP/G015325/1 which includes a 50% MoD(UK) contribution (JGS 1194), The Croatian Ministry of Science, Education and Sports, project No. 098-0982934-2717 and North Atlantic Treaty Organization (NATO) Science for Peace (SfP) Award Reference 983147. IPgroup PLC funded JM with a "grub fund" award.

References

1. Nelson A, Benton A (1986) J Electroanal Chem 202:253
2. Nelson A, Auffret N (1988) J Electroanal Chem 244:99
3. Leermakers FAM, Nelson A (1990) J Electroanal Chem 278:53
4. Nelson A, Leermakers FAM (1990) J Electroanal Chem 278:73
5. Nelson A (2001) Biophys J 80:2694
6. Moncelli MR, Becucci L, Nelson A et al (1996) Biophys J 70:2716
7. Nelson A (1987) Anal Chim Acta 194:139
8. Guidelli R, Becucci L, Dolfi A et al (2002) Solid State Ionics 150:13
9. Coldrick Z, Steenson P, Millner P et al (2009) Electrochim Acta 54:4954
10. Stoodley R, Bizzotto D (2003) Analyst 128:552
11. Ross JW, Demars RD, Shain I (1956) Anal Chem 28:1768
12. Thompson M, Krull UJ (1982) Anal Chim Acta 141:33
13. Thompson M, Krull UJ, Bendell-Young LI (1983) Talanta 30:919
14. Thompson M, Krull UJ, Wong HE (1986) Bioelectrochem Bioener 15:371
15. Diederich A, Bahr G, Winterhalter M (1998) Phys Rev E 58:4883
16. Kitta M, Tanaka H, Kawai T (2009) Biosens Bioelectron 25:93
17. Knoll W, Koper I, Naumann R et al (2008) Electrochim Acta 53:6680
18. Ogier SD, Bushby RJ, Cheng Y et al (2001) In: Sood DK, Lawes RA, Varadan VV (eds) Smart structures and devices. Proceedings of the society of photo-optical instrumentation engineers (SPIE), vol 4235. Society of Photo-Optical Instrumentation Engineers, Bellingham, p 452
19. Millo D, Bonifacio A, Sergo V et al (2010) Colloid Surf B 81:212
20. Cornell BA, Krishna G, Osman PD et al (2001) Biochem Soc Trans 29:613
21. Woodhouse G, King L, Wieczorek L et al (1999) J Mol Recognit 12:328
22. Nelson A (2010) Curr Opin Colloid Interface Sci 15:455
23. Ringstad L, Protopapa E, Lindholm-Sethson B et al (2008) Langmuir 24:208
24. Protopapa E, Maude S, Aggeli A et al (2009) Langmuir 25:3289
25. Kasem KK, Jones S (2008) Platinum Met Rev 52:100
26. Han J-H, Park S, Boo H et al (2007) Electroanal 19:786
27. Bott AW (1995) Curr Sep 14:64
28. Sessa G, Weissmann G (1968) J Lip Res 9:310
29. Bizzotto D, Nelson A (1998) Langmuir 14:6269
30. Hellberg D, Scholz F, Schauer F et al (2002) Electrochem Commun 4:305
31. Hernández VA, Hermes M, Milchev A et al (2009) J Solid State Electrochem 13:639
32. Nelson A (2007) J Electroanal Chem 601:83
33. Brukhno AV, Akinshina A, Coldrick Z et al (2011) Soft Matter (in press). doi:10.1039/c0sm00724b
34. Bond AM (1994) Analyst 119:R1
35. Nelson A, Auffret N, Readman J (1988) Anal Chim Acta 207:45
36. Nelson A, Auffret N, Borlakoglu J (1990) Biochim Biophys Acta 1021:205
37. Bruggeman WA, van der Steen J, Hutzinger O (1982) J Chromatogr 238:335
38. Harner T, Mackay D (1995) Environ Sci Technol 29:1599
39. Kozuka H, Yamada J, Horie S, Watanabe T, Suga T, Ikeda T (1991) Biochem Pharmacol 41:617
40. Hofmann D, Hartmann F, Herrmann H (2008) Anal Bioanal Chem 391:161